JPL PUBLICATION 82-75

Basic Investigation Into the Electrical Performance of Solid Electrolyte Membranes

Robert Richter

August 15, 1982

NASA
National Aeronautics and Space Administration

Jet Propulsion Laboratory
California Institute of Technology
Pasadena, California

JPL PUBLICATION 82-75

Basic Investigation Into the Electrical Performance of Solid Electrolyte Membranes

Robert Richter

August 15, 1982

National Aeronautics and
Space Administration

Jet Propulsion Laboratory
California Institute of Technology
Pasadena, California

The research described in this publication was carried out by the Jet Propulsion Laboratory, California Institute of Technology, under contract with the National Aeronautics and Space Administration.

TABLE OF CONTENTS

LIST OF ILLUSTRATIONS

LIST OF TABLES

ABSTRACT

The electrical performance of solid electrolyte membranes is being investigated analytically and the results are compared with experimental data. It is concluded that in devices that are used for pumping oxygen the major power losses have to be attributed to the thin film electrodes. Relations have been developed by which the effectiveness of tubular solid electrolyte membranes can be determined and the optimum length evaluated. The observed failure of solid electrolyte tube membranes in very localized areas is now being explained by the highly non-uniform current distribution in the membranes. The analysis points to a possible contact resistance between the electrodes and the solid electrolyte material. This possible contact resistance remains to be investigated experimentally. It is concluded that film electrodes are not appropriate for devices which operate with current flow, i.e., pumps, though they can be employed without reservation in devices that measure oxygen pressures if a limited increase in the response time can be tolerated.

SECTION I

INTRODUCTION

The two most difficult problems confronting the development of an oxygen extraction device are the sealing of the membranes and the application of electrodes to the solid electrolyte membrane surface. The membrane has to be configured for perfect gas sealing, while the electrodes have to operate with low electrical losses and minimal flow obstruction to oxygen flow. The reported effort investigates analytically the electrical circuitry of an oxygen extraction device. The performance of a solid electrolyte tube membrane which uses platinum thick film electrodes on both inner and outer surface is evaluated. A device of this design was tested and produced data from which a considerable amount of electrical performance data could be extracted. The probable characteristics of electrodes constructed with a platinum thick film are presented. The conclusions which are drawn are based on the analysis and a comparison of the analytically developed parametric relations with experimental data.

In the solid electrolyte oxygen extraction device the electrode has to be spread over the entire solid electrolyte membrane since electrical current has to be conducted to and from the whole surface. While presenting a low electrical resistance parallel to the surface of the membrane, the electrode has also to be permeable to the oxygen which is being pumped across the solid electrolyte. To insure that a thick film electrode, which is presently the only known electrode configuration, is porous from the start of the operation and will not lose its permeability to gas flow due to sintering, only a relatively thin film of platinum can be applied over the solid electrolyte substrate. This type of electrode design has proven acceptable for oxygen pressure sensors, which measure solely an electrical potential without current or gas flow flow. However, since in an oxygen extraction device electric current has to be conducted parallel to the membrane face, the electrodes have to be relatively thick to prevent large voltage drops and electric power dissipation. Thus it becomes evident that the two main requirements for an electrode in a solid electrolyte oxygen extraction device, i.e., high electrical conductivity and gas permeability, are not achievable concurrently with a thick film electrode as they are mutually exclusive. The solution to these two opposing requirements for the electrode is shown conclusively to be a necessary prerequisite for the efficient electrical performance of the extraction device.

A new electrode design which will combine low electrical resistance with high gas permeability has to be explored (Ref.1). The proposed electrode design uses knitted or woven platinum

cloth which is imbedded into the surface of the solid electrolyte material. The knitted wire cloth is called for when applied as a sock over a tubular solid electrolyte membrane. The woven wire cloth is more applicable to flat solid electrolyte membranes. The electrical conductivity of this type of an electrode can easily be controlled by the mesh size and the wire diameter of the cloth without affecting permeability. Furthermore, the electrode will remain permeable throughout its lifetime as no sintering occurs which is a common process in the thick film electrode that leads to an increase in resistance to gas flow with time of operation.

But before it can be concluded that the proposed integrated electrode design will produce the desired lower electric power dissipation, the electrical operation of an oxygen extraction device had to be analyzed. The analytically derived relations permit the determination of contact resistances which might prove to be an additional resistance in the electric circuit of the electrode covered solid electrolyte membrane. This resistance has not been recognized yet and its absolute value and parametric dependencies are unknown.

SECTION II

ELECTRICAL ANALYSIS

2.1 Electrical Circuit Components

The two major electric circuit components of an oxygen extraction device are the electrodes and the solid electrolyte membrane. In addition to the physical components, overpotentials and contact resistances contribute to voltage drops in the electrical circuit. This investigation is primarily concerned with the evaluation of the voltage drops associated with the electrodes which cover the surface of the solid electrolyte membrane. In the oxygen extraction device the solid electrolyte membrane is made of 8% by mole yttria stabilized zirconia which permits the selective conduction of oxygen ions through its matrix. The electrodes have up to the present time been platinum thick films which are applied in the form of a paste of suspended platinum particles in a carrier to the oxide membrane.

2.1.1 Platinum Thick Film

For the construction of a platinum thick film electrode two types of platinum ink are available, the fritted and the fritless ink. The fritted ink contains glass which provides fusion type bonding of the fired platinum film with the substrate. The fritless type ink produces a film which after firing in an oxygen atmosphere is bonded to the oxide substrate by reaction bonding, a process which is not well understood yet.

The two types of ink produce not only films which differ in their bonding to the substrate but which also exhibit different electrical resistivity. Generally the electrical resistivity of a thick film is expressed by a value whose dimensions are milliohms per square, i.e., the electrical resistance along a length of a square thick film which has a thickness of 0.001 inch. This value can be converted to the standard resistivity ρ(ohm-cm) of the film material by multiplying it by 2.54×10^{-3}. Typical room temperature resistance values for thick films produced by platinum ink are found in the catalog of Thick Film, Inc. as presented in Table 1.

Ink Type		Resistivity R_f mohm/square	Effective Resistivity ρ_f ohm-cm
Fritless	4082	20 - 30	50×10^{-6} - 76×10^{-6}
Fritted	3804	33 - 37	83×10^{-6} - 94×10^{-6}

Table 1 Resistivity of Thick Film Electrode Materials

The resistivity of the platinum thick film materials can be compared with the room temperature resistivity of pure solid platinum which is

$$\rho_p = 10 \times 10^{-6} \text{ ohm-cm}$$

The resistivity of pure solid platinum as a function of temperature is shown in Figure 1. Though no resistivity data of thick films in the temperature range of interest, i.e., 1000°C, are available, it must be assumed that thick films will exhibit an increase in resistivity with temperature similar to that of pure platinum. Thus, one has to expect that even a thick film, when constructed with fritless ink, would present a resistance of about five times that of solid platinum at the operating temperature of the solid electrolyte.

2.1.2 Membrane Configuration

For an oxygen extraction device three membrane configurations can be envisioned: rectangular, round and tubular. The rectangular and round configurations permit the design of the most compact device. Construction of an oxygen extraction device with round membranes was actually attempted by several investigators. However, sealing of the membranes could not be achieved. The stresses which are generated by the differential thermal expansion of the materials and the temperature distributions cannot be accommodated by presently known metal to ceramic seals that can function at the required operating temperature of 1000°C.

At the present time sealing of the membranes can be achieved when the seals are moved from the high temperature region to a location which permits the application of known low temperature sealing processes. This selective relocation of the sealing surfaces can only be accomplished with tubular solid electrolyte membranes as shown in Figure 2.

The tubular membrane consists of a solid electrolyte tube which is closed on one end. Both inside and outside surfaces are coated with a thick film made of platinum ink. The carbon dioxide - carbon monoxide - oxygen gas mixture flows along the outside surface while the oxygen is selectively conducted to the inside in the ionic state across the solid electrolyte membrane under the influence of an applied electrical potential. The two required seals are located at the open end of the tube which extends to the outside of the heated thermally insulated enclosure which surrounds the closed end of the tube.

Previously the process for extracting oxygen from carbon dioxide in a solid electrolyte device was analyzed considering the thermodynamic, kinetic and electrochemical aspects of the process. Test data which were generated during the experimental

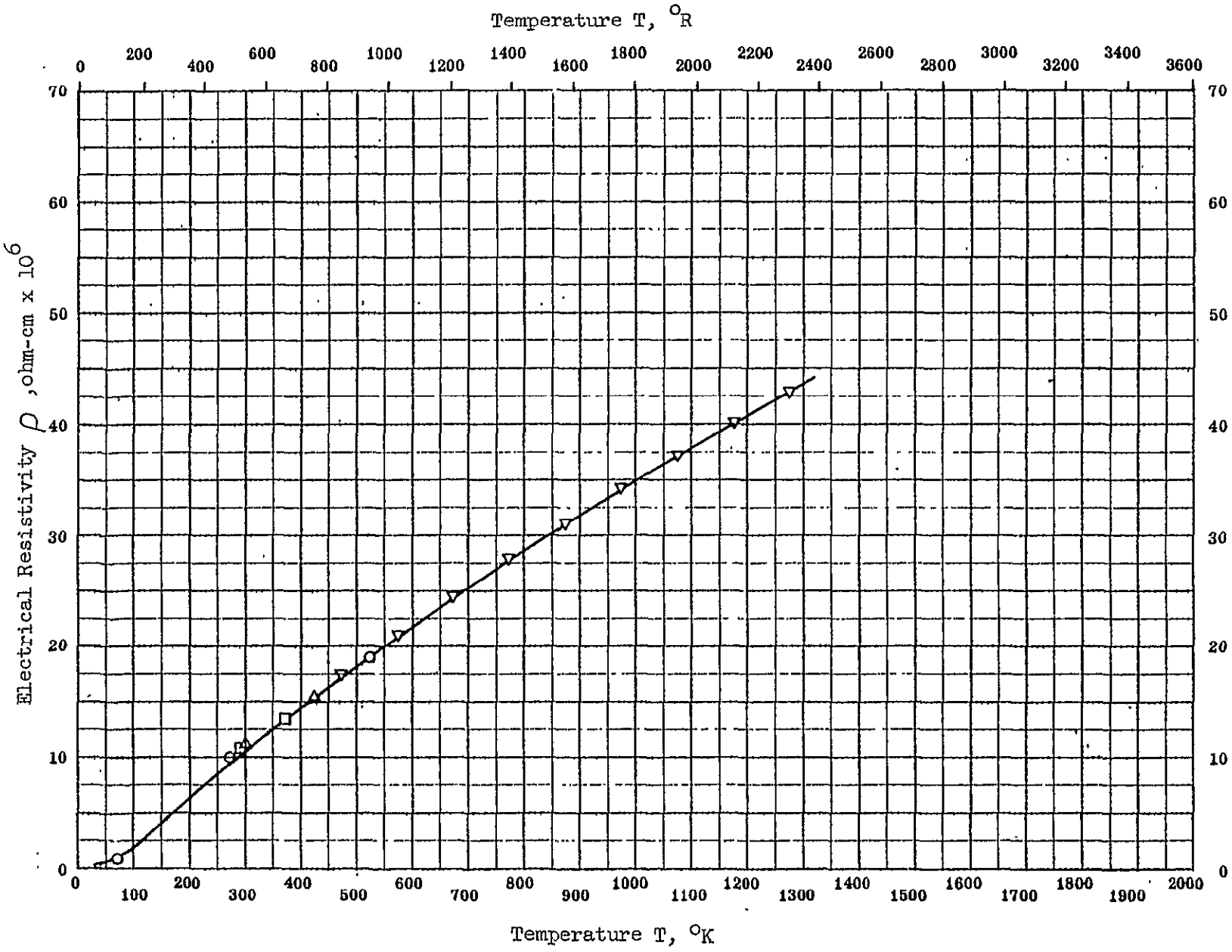

Figure 1 Electrical Resistivity of Platinum

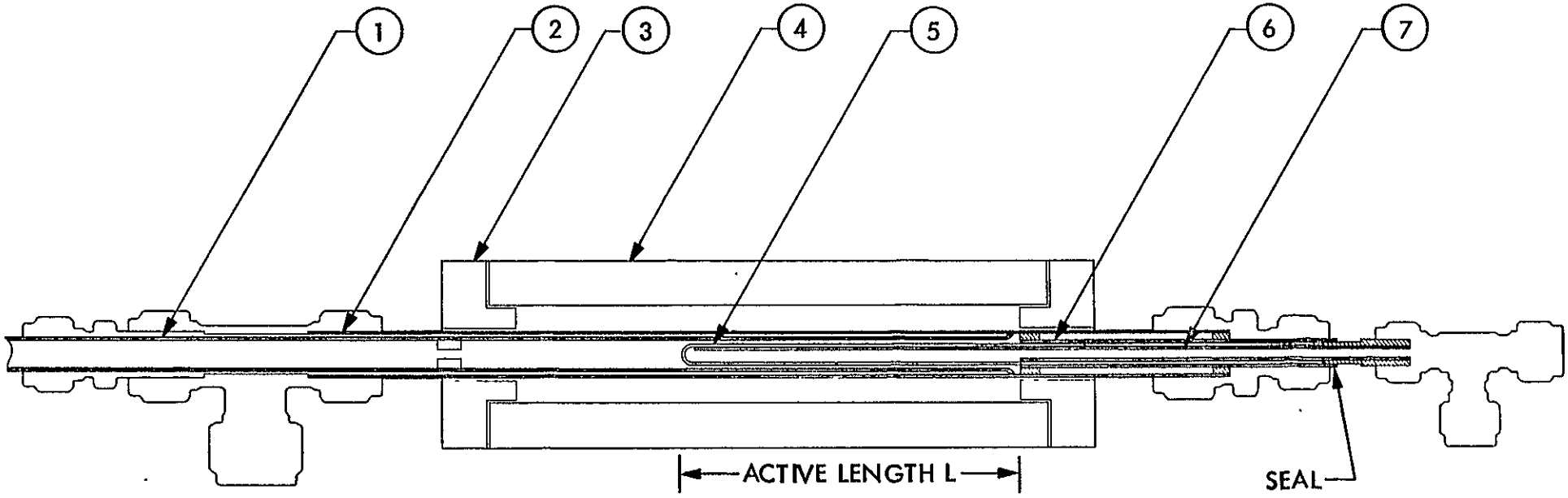

1. INCONEL 600 TUBING 3/8-in. x 0.035 in. WALL
2. INCONEL 600 TUBING 1/2-in. x 0.035 in. WALL
3. BORON NITRIDE SLEEVE (2)
4. HEATER, LINDBERG MODEL 50012 TYPE 74-KS (2)
5. 8% YTTRIA STABILIZED ZIRCONIA TUBE WITH 0.005 in. PLATINUM COAT ON BOTH SIDES 0.261 in. x 0.058 in. WALL
6. INCONEL 600 TUBING 3/8-in. x 0.058 in. WALL
7. INCONEL 600 TUBING 0.166-in. x 0.004 in. WALL

Figure 2 Electrolytic Cell Design With Tube Membrane

phase of the program were shown to agree fully with the analytical predictions (Ref.2). The basic relation

$$V_T = E(\dot{W}_{CO_2}, p_{O_21}, p_{O_22}, T_o, s) + E_o + (R_s + R_z)i \quad (1)$$

where

V_T	total applied voltage, volt
E	pressure potential, volt
$\dot{W}_{CO_2}$	CO_2 flow rate, SCCM
p_{O_21}	supply partial pressure of O_2, atm
p_{O_22}	product partial pressure of O_2, atm
s	flow resistance, atm/(ampere/cm^2)
T_o	operating temperature, K
E_o	ionization overpotential, volt
R_s	surface resistance, ohm-cm^2
R_z	membrane resistance, ohm-cm^2
i	current density, ampere/cm^2

was shown to satisfy all test data. The thermodynamic analysis was primarily concerned with the parametric relation of the pressure potential E as a function of the operating parameters, temperature, supply pressure, product pressure, flow rate and flow resistance of the electrodes. The overpotentials associated with the ionization and the electrode resistance were extracted from the test data and remained to be investigated in future analyses and special test programs.

The electrical analysis of this report investigates the influence of the electrode characteristics and attempts to characterize the thick film electrodes when operating at the high temperature of an oxygen extraction device.

2.2 Electrode Characteristics

Electrodes of an oxygen extraction device distinguish themselves by two characteristics, the electrical characteristic, which is concerned with the electrical resistance to current flow parallel to the face of the solid electrolyte membrane, and the flow characteristic which influences the effective oxygen pressure on the CO_2-CO-O_2 gas mixture side. The flow characteristic and its effect on the thermodynamic cycle of the oxygen extraction device have been analyzed in Ref.2. The electrical characteristic of the electrode and its effects on the electric circuit

with respect to voltage drop and power dissipation are investigated in this report.

2.2.1 Experimental Evaluation of Surface Resistance

The basic relation

$$V_T = E(\dot{W}_{CO_2}, p_{O_21}, p_{O_22}, T_o, s) + E_o + (R_s + R_z)i \qquad (1)$$

indicates that the total voltage V_T is the sum of two types of electric circuit components, components which are dependent and components which are independent on the current density i. By operating the extraction device in two modes, one mode at which the independent components remain constant, and the other mode at which both components vary with changes in the applied voltage V_T, a sufficient number of relations were established for evaluating the absolute value of each component. The test data shown in Figure 3 established a total resistance R_T

$$R_T = 23.73 \text{ ohm-cm}^2$$

where $$R_T = R_z + R_s \qquad (2)$$

and $$R_z = \rho_z t_z \qquad (3)$$

With the resistivity ρ_z of the solid electrolyte material and the thickness t_z of the membrane known, a surface resistance R_s

$$R_s = 22.94 \text{ ohm-cm}^2$$

could be evaluated. This surface resistance remained constant under all operating conditions.

2.2.2 Analytical Evaluation of the Surface Resistance

The electrical current flows from a potential $+V_o$ to a potential $-V_o$ through the electrode and the solid electrolyte membrane in a membrane configuration as shown in Figure 4.

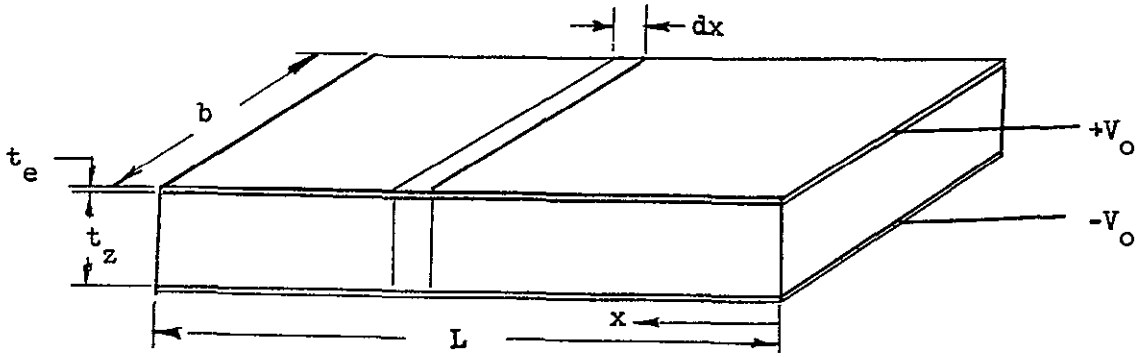

Figure 4 Solid Electrolyte Membrane Configuration

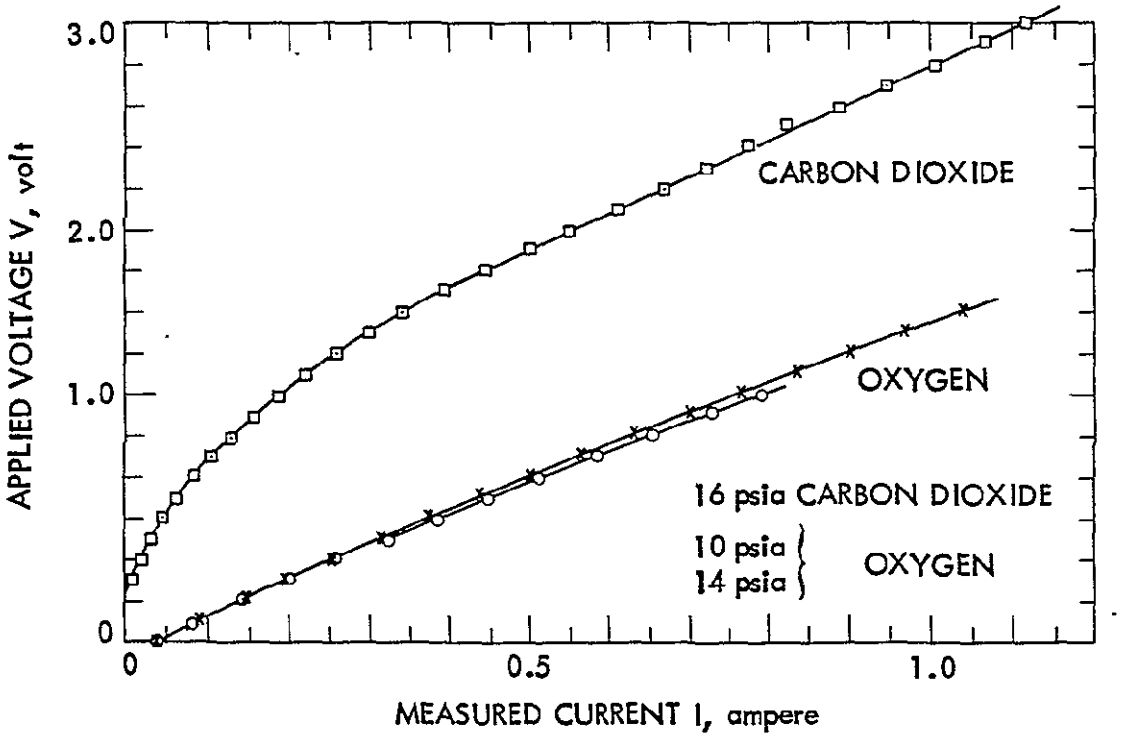

Figure 3 Measured Voltage - Current Relations of a Single Tube Membrane Oxygen Extraction Device

The width b of the membrane is equal to the circumference of the solid electrolyte tube, i.e.,

$$b = \pi D_t \tag{4}$$

where D_t effective tube diameter, cm

Three basic relations which govern the electrical circuit as shown in Figure 4 can be formulated.

1. The current density at which oxygen ions flow through the membrane at a distance x is

$$i = 2(V_o - V)/R_z \tag{5}$$

where V voltage drop along the electrode distance x, volt

2. The change in voltage drop along the electrode as determined by the electrical resistance and the current flow is

$$dV = (R_e I/b)dx \tag{6}$$

where I current flow in the electrode at x, ampere

R_e electrode resistance, ohm

$$R_e = \rho_e/t_e \tag{7}$$

3. The change in current flowing through the electrode as determined by the current flowing through the membrane is

$$dI = -ibdx \tag{8}$$

In addition to the three basic relations given above, the electrical circuit operates with the following boundary conditions:

1. The current flow in the electrode at the closed tube end is zero.

$$x = L: \quad I = 0$$

2. The entire current flows through the electrode at the open end of the tube.

$$x = 0: \quad I = I_T$$

3. The entire current flowing through the solid electrolyte membrane is equal to the total current flow.

$$I_T = \int_0^L ibdx \tag{9}$$

When the voltage drop V is non-dimensionalized by the applied voltage V_o, relations 5 and 6 can be written

$$i = 2V_o(1 - v)/R_z \tag{10}$$

and

$$dv = (R_e I/V_o b)dx \tag{11}$$

where

$$v = V/V_o$$

Furthermore if a parameter τ is defined by

$$\tau = 1 - v \tag{12a}$$

and

$$-dv = d\tau \tag{12b}$$

then relation 10 can be written as

$$i = 2V_o\tau/R_z \tag{13}$$

When the current density i in relation 8 is replaced by relation 13, the change in current is expressed by

$$dI = -(2V_o\tau b/R_z)dx \tag{14}$$

By dividing relation 11 by relation 14, separating the variables and using relation 12b

$$\tau d\tau = (R_e R_z/2V_o^2 b^2)IdI \tag{15}$$

By integration of relation 15 over the limits

$V = 0$: $v = 0$, $\tau = 1$, $I = I_T$

$V = V_L$: $v = v_L$, $\tau = \tau_L$, $I = 0$

$$1 - \tau_L^2 = (R_e R_z/2b^2V_o^2)I_T^2 \tag{16}$$

Solving relation 16 for the total current I_T produces

$$I_T = (1 - \tau_L^2)^{1/2}(2/R_e R_z)^{1/2} bV_o \tag{17a}$$

or

$$I_T/(2V_o Lb/R_z) = (1 - \tau_L^2)^{1/2}(R_z/2R_e)^{1/2}/L \tag{17b}$$

If a characteristic length L_c is defined by

$$L_c = (R_z/2R_e)^{1/2} \tag{18}$$

then

$$I_T/(2V_oLb/R_z) = (1 - \tau_L^2)^{1/2}/(L/L_c) \tag{17c}$$

By integration of relation 15 over the limits

$$V = V: \quad v = v, \quad \tau = \tau, \quad I = I$$

$$V = V_L: \quad v = v_L, \quad \tau = \tau_L, \quad I = 0$$

$$\tau^2 - \tau_L^2 = (R_eR_z/2V_o^2b^2)I^2 \tag{19a}$$

or

$$I/(2V_oLb/R_z) = (\tau^2 - \tau_L^2)^{1/2}/(L/L_c) \tag{19b}$$

Differentiation of relation 19b results in the relation

$$(L/L_c)dI/(2V_oLb/R_z) = \{\tau(\tau^2 - \tau_L^2)^{-1/2}\}d\tau \tag{20}$$

and substituting relation 14 into relation 20 produces relation

$$-(L/L_c)d(x/L) = (\tau^2 - \tau_L^2)^{-1/2}d\tau \tag{21}$$

By integration of relation 21 between the limits

$$x = x: \quad V = V, \quad v = v, \quad \tau = \tau$$

$$x = L: \quad V = V_L, \quad v = v_L, \quad \tau = \tau_L$$

$$(L/L_c)(1 - x/L) = \ln\{\tau_L/[\tau + (\tau^2 - \tau_L^2)^{1/2}]\} \tag{22}$$

With the known boundary conditions

$$x = 0: \quad V = 0, \quad v = 0, \quad \tau = 1$$

$$-L/L_c = \ln\{\tau_L/[1 + (1 - \tau_L^2)^{1/2}]\} \tag{23}$$

or

$$\tau_L = 1/\cosh(L/L_c) \tag{24}$$

When solving relation 22 for the voltage parameter τ, the potential drop along the electrode is determined as a function of the distance from the end of the tube as shown by relation 25

$$\tau = \tau_L \cosh\{(L/L_c)(1 - x/L)\} \tag{25}$$

By substituting the total voltage drop τ_L as given by relation 24 into relation 25, the voltage paramter τ is expressed by

$$\tau = \cosh\{(L/L_c)(1 - x/L)\}/\cosh(L/L_c) \tag{26}$$

When the value of τ as expressed by relation 26 is inserted into relation 13, the current density distribution along the length of the tubular solid electrolyte membrane is found to be

$$i/(2V_o/R_z) = \cosh\{(L/L_c)(1 - x/L)\}/\cosh(L/L_c) \tag{27}$$

The total current which is carried across the membrane is from relations 17c and 24

$$I_T/(2V_oLb/R_z) = \{1 - 1/\cosh^2(L/L_c)\}^{1/2}/(L/L_c) \tag{28a}$$

or

$$I_T = (2V_oLb/R_z)\{\tanh(L/L_c)\}/(L/L_c) \tag{28b}$$

With the establishment of the relation between the total current I_T and the applied potential $2V_o$ as a function of the effective surface resistance as defined by the relation

$$2V_o = (R_{sV} + R_z)i_e \tag{29}$$

where

R_{sV} surface resistance based on voltage drop, ohm-cm^2

i_e effective current density, ampere/cm^2

and

$$i_e = I_T/Lb \tag{30}$$

or

$$i_e = (2V_o/R_z)\{\tanh(L/L_c)\}/(L/L_c) \tag{31}$$

the membrane characteristic L/L_c can be evaluated from experimental data.

When relation 31 is substituted into relation 29 the surface resistance R_{sV} can be calculated from known values by relation 32

$$R_{sV} = R_z\{(L/L_c)/\tanh(L/L_c) - 1\} \tag{32}$$

The surface resistance R_{sV} corresponds to the electric circuit value as defined by relation 29, i.e., a resistance which is in series with the solid electrolyte membrane resistance and thus determines the total current I_T for a given applied voltage $2V_o$. Another surface resistance R_{sP} can be defined which is based on the electric power dissipation P_e in the electrode.

The electric power dissipation associated with the surface resistance R_{sP} is found by integration of the electrode loss over the length L.

$$P_e = 2\int_0^L (I^2 R_e/b)dx \tag{33}$$

Replacing the current I of relation 19b in relation 33 and using relations 24 and 26, relation 33 becomes

$$P_e = (4V_o^2 b\tau_L^2/R_z)\int_0^{L/L_c} (\cosh^2 u - 1)du \tag{34}$$

where $$u = (L/L_c)(1 - x/L) \tag{35a}$$

and $$du = -dx/L_c \tag{35b}$$

For the limits:

$$x = 0: \quad u = L/L_c$$

$$x = L: \quad u = 0$$

$$P_e = \{(2V_o)^2 Lb/R_z\}\{[\tanh(L/L_c)]/(L/L_c) - 1/\cosh^2(L/L_c)\}/2 \tag{36}$$

Relation 36 permits the evaluation of the electric power dissipation in the electrodes with electric circuit values which are known from basic material data or which can be evaluated from a measured correlation between total current I_T and applied voltage $2V_o$.

A surface resistance R_{sP} can now be defined by the power dissipation P_e in the electrodes and the total current I_T by

$$P_e = I_T^2 R_{sP}/Lb \tag{37}$$

The power loss P_e of relation 36 can be equated with the power loss P_e of relation 37 and the resulting relation can be solved for the surface resistance R_{sP} to produce

$$R_{sP} = (R_z/2)\{(L/L_c)/\sinh(L/L_c)\}^2\{[\sinh 2(L/L_c)]/2(L/L_c) - 1\} \tag{38}$$

When the two surface resistances R_{sV} (relation 32) and R_{sP} (relation 38) are compared, it is seen that they are not equal. This clearly indicates that the effective surface resistance based on the voltage drop in the electric circuit cannot be used to evaluate the electric power dissipation by relation 37 using the surface resistance R_{sV} which was evaluated from the voltage drop.

The electrode resistance as was defined by

$$R_e = \rho_e / t_e \tag{7}$$

can now be evaluated from experimental data by relation 18 which can be solved for R_e

$$R_e = R_z (L/L_c)^2 / 2L^2 \tag{39}$$

where according to relations 32

$$L/L_c = f(R_{sV}/R_z) \tag{41}$$

The total electric power dissipation P_T is the sum of the losses in the membrane and the electrode

$$P_T = P_e + P_z \tag{42}$$

while also being the product of the applied voltage $2V_o$ and the total current I_T

$$P_T = 2V_o I_T \tag{43}$$

Substituting the total current I_T as given by relation 28 into relation 43 the total power loss is

$$P_T = \{(2V_o)^2 Lb/R_z(L/L_c)\}\tanh(L/L_c) \tag{44}$$

When the electrode loss P_e as given by relation 36 is subtracted from the total power loss P_T as given by relation 44, the electric power dissipation P_z in the solid electrolyte membrane is found to be

$$P_z = \{(2V_o)^2 Lb/R_z\}\{[\tanh(L/L_c)]/(L/L_c) + \cosh^{-2}(L/L_c)\}/2 \tag{45}$$

It is interesting to observe by comparing the electrode loss P_e and the membrane loss P_z that the electrode loss will never exceed the membrane loss and that with increasing length parameter L/L_c the two losses become equal.

2.3 Application of Analysis to Experimental Data

The analysis has produced the basic relations by which the interaction of the various parameters affecting the electrical operation of an oxygen extraction device can be evaluated. The results can now be employed to establish the actual characteristics of the electrical components of the device from experimental data.

From the data shown in Figure 3 the total resistance R_T

$$R_T = R_{sV} + R_z$$

was found to be

$$R_T = 23.73 \text{ ohm-cm}^2$$

when the device was operated at a temperature $T_o = 1273K$. At that temperature the oxygen ion resistivity of the solid electrolyte material is from Ref.3

$$\rho_z = 9.69 \text{ ohm-cm}$$

With a membrane thickness

$$t_z = 0.0813 \text{ cm}$$

the membrane resistance R_z was

$$R_z = 0.7878 \text{ ohm-cm}^2$$

The above values indicate that only about 3.32 percent of the total resistance was associated with the solid electrolyte membrane and that the surface resistance based on the voltage drop was

$$R_{sV} = 22.94 \text{ ohm-cm}^2$$

From relation 32, which is plotted in Figure 5, the length parameter L/L_c has to be

$$L/L_c = 30.3$$

For a length $L = 9.021$ cm the electrode resistance is found from relation 39 to be

$$R_e = 4.444 \text{ ohm}$$

which could also be obtained directly from Figure 6. The effective resistivity ρ_e of the electrode material can be found from relation 7

$$\rho_e = 4.444 \; t_e(\text{cm})$$

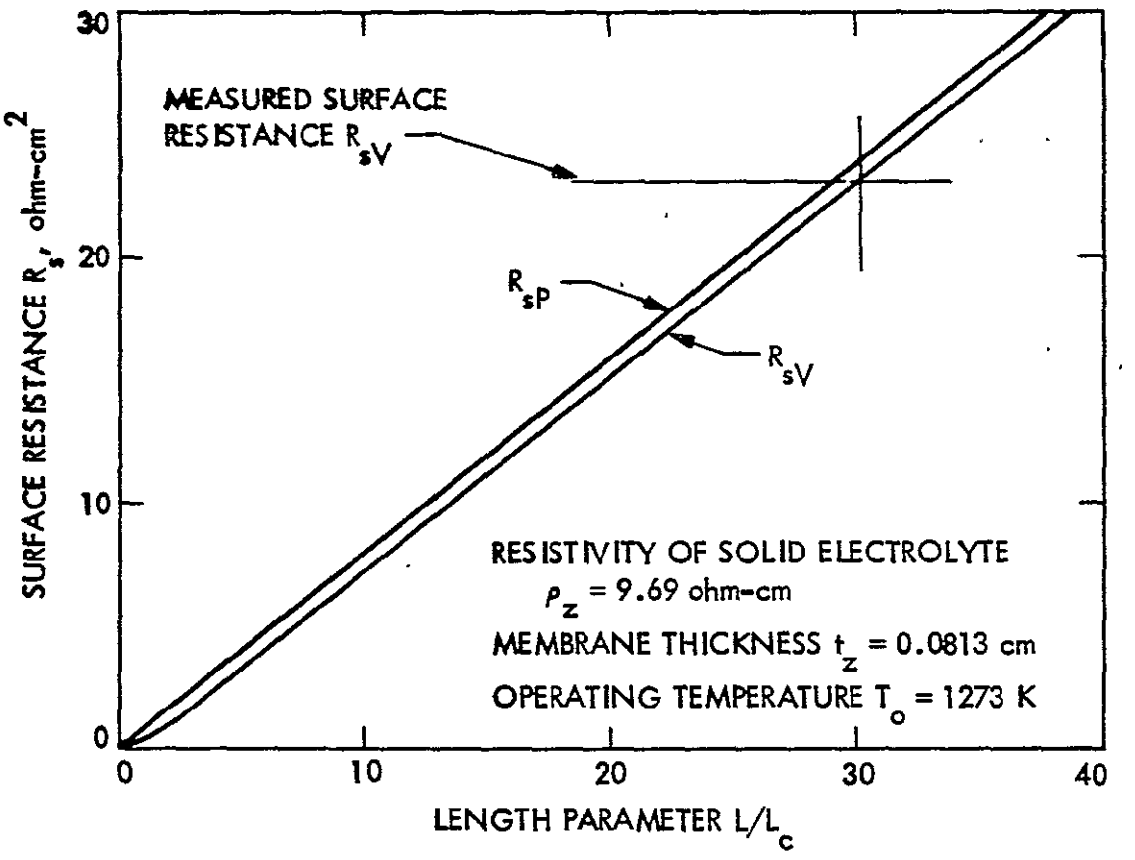

Figure 5 Correlation Between Length Parameter and Effective Surface Resistance

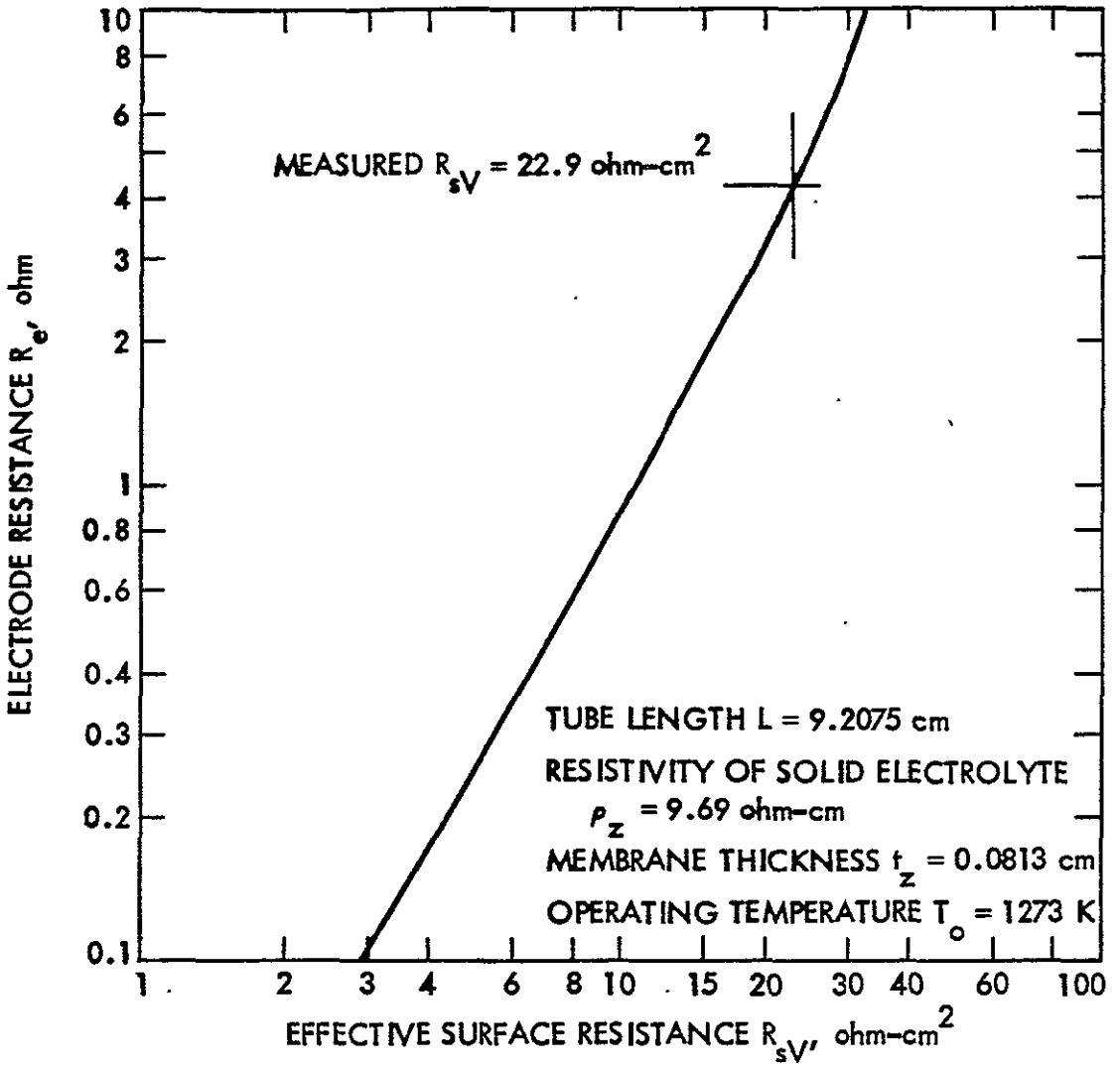

Figure 6 Relation Between Effective Surface Resistance and Electrode Resistance

$$\rho_e = 11.29 \times 10^{-3}\ t_e(10^{-3}\ \text{inch})$$

The relation between resistivity ρ_e and thickness t_e is plotted in Figure 7. Since the thickness of the thick film was on an average $t_e = 1.5$ mils, the indicated resistivity of the film material was about

$$\rho_{ef} = 16.935 \times 10^{-3}\ \text{ohm-cm}$$

This value compares with a resistivity of about

$$\rho_e = 0.35 \times 10^{-3}\ \text{ohm-cm}$$

which is obtained by multiplying the room temperature resistivity of the fritless platinum film material by the same factor by which the platinum resistivity increases when heated from room temperature to 1273K. Thus the actual hot resistivity of the film material as determined by the test data is 54 times that which would have been predicted from the published room temperature resistivity data.

If the electrode resistivity were about of the predicted magnitude

$$\rho_e = 102 \times 10^{-6}\ \text{ohm-cm}$$

the resistance R_e for a film thickness $t_e = 1$ mil would be

$$R_e = 40.16 \times 10^{-3}\ \text{ohm}$$

the characteristic length

$$L_c = 3.132\ \text{cm}$$

and the length parameter for the 9.021 cm long tube membrane

$$L/L_c = 2.88$$

Even with the ideal predicted electrode resistivity the solid electrolyte membrane would still operate only with an effectiveness of about 33.1%, as can be seen from Figure 8. The membrane would carry only one third of the current which could be conducted by a membrane that had an integrated electrode with a resistance of one tenth of that of the ideal film electrode.

The analysis has shown that the current density along the tube membrane is not uniform, but varies substantially along the length. Figure 9 shows the current density distributions for four tubes which have the same total resistance R_T and the same characteristic length L_c but vary solely in their total length. Table 2 presents the current density distribution which was experienced by the experimental tube membrane. The analytical

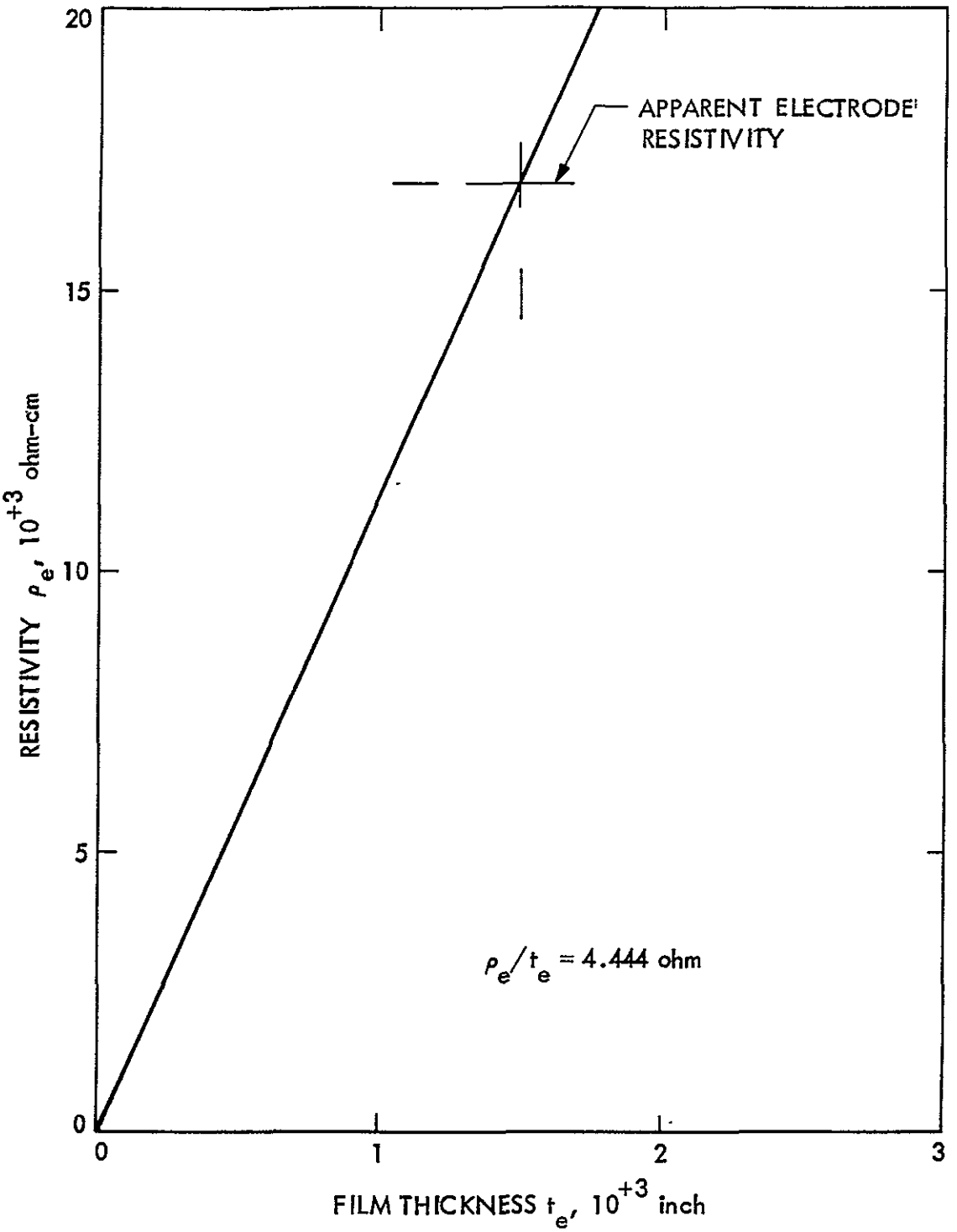

Figure 7 Combination of Film Thickness and Resistivity of Film Material as Indicated by Test Data

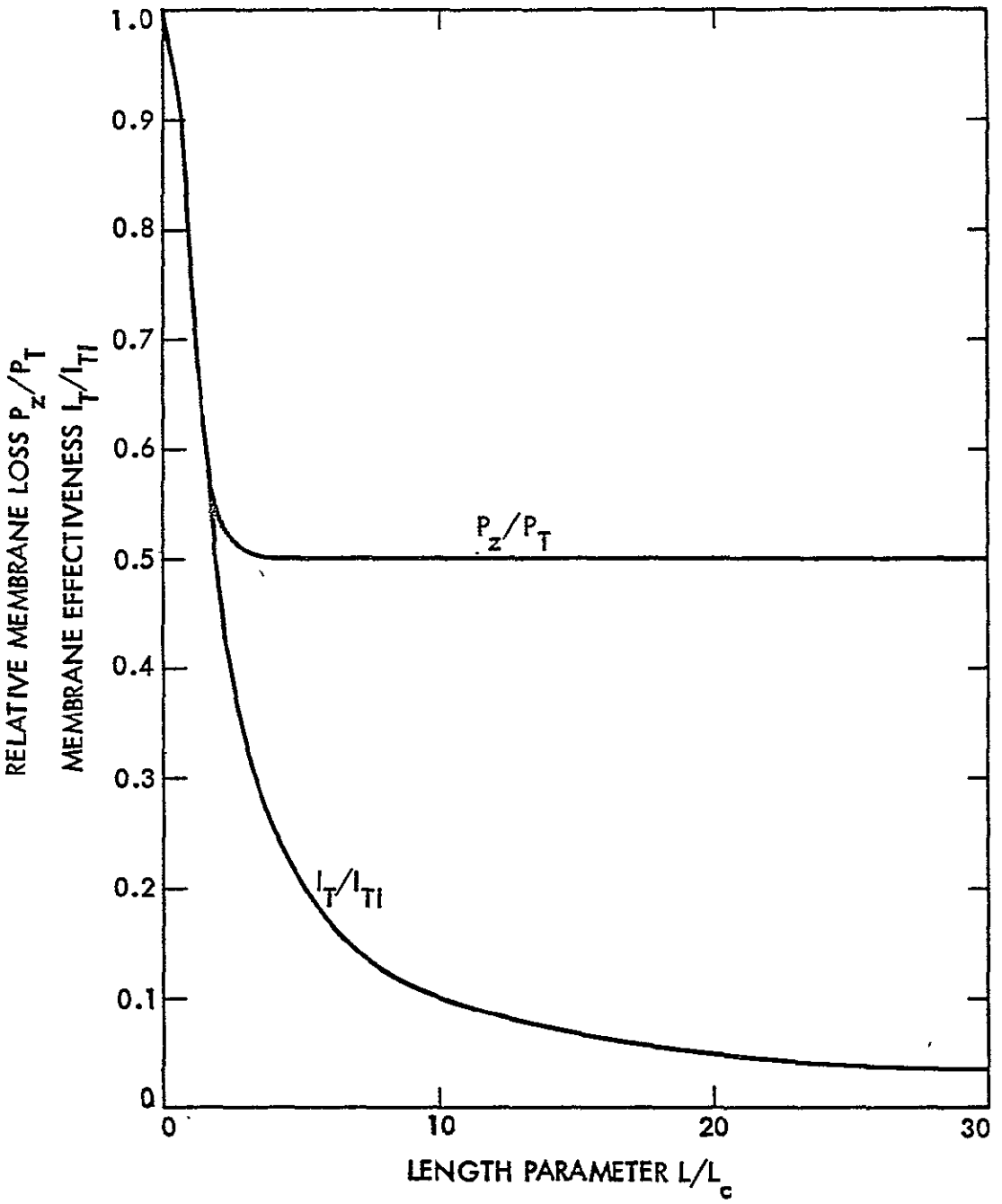

Figure 8 Tube Membrane Effectiveness as Determined by the Length Parameter

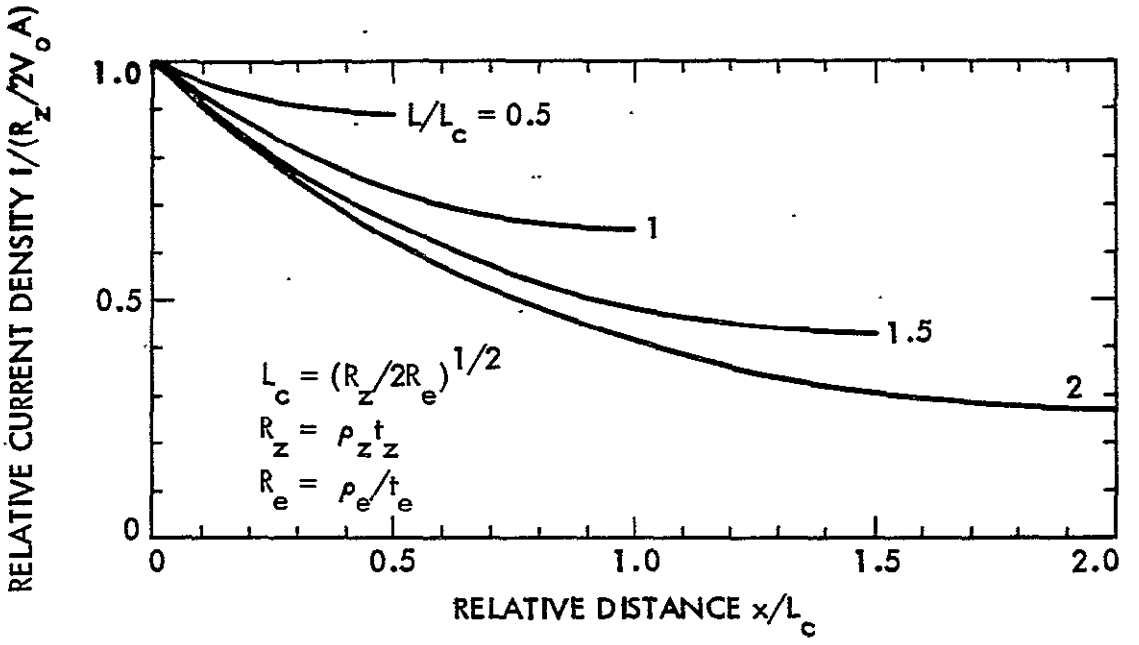

Figure 9 Current Density Distribution in Solid Electrolyte Tube Membrane

results clearly indicate that the tube membrane operated highly ineffectively. Only a very short section of the tube carried the entire current at a relatively high current density. Furthermore, only one thirtieth of the total current was conducted when compared with a tube membrane whose surface resistance is zero.

REL.LENGTH	TOTAL CURRENT	MEMBRANE LOSS	ELECTRODE LOSS
30.3	.0330033	.5	.5

RELATIVE DISTANCE x/L	RELATIVE CURRENT DENSITY
0	1
.05	.219809
.1	.0483157
.15	.0106202
.2	2.33441E-03
.25	5.13121E-04
.3	1.12788E-04
.35	2.47918E-05
.4	5.44943E-06
.45	1.19783E-06
.5	2.63293E-07
.55	5.7874E-08
.6	1.27212E-08
.65	2.79621E-09
.7	6.14631E-10
.75	1.35101E-10
.8	2.96965E-11
.85	6.52822E-12
.9	1.43814E-12
.95	3.30618E-13
1	1.38646E-13

Table 2 Current Density Distribution in an Experimental Solid Electrolyte Tube Membrane (L = 9.021 cm)

The analytically determined current density distribution in the tube membrane can now explain the failure mode of tube membranes which was observed by Life Systems, Inc. when operating the same type of tube membrane at high applied voltage potentials. Failure due to reduction of the solid electrolyte material occurred entirely and exclusively at the upper end of the tube. Whenever the voltage exceeded the critical potential, the critical potential being the potential that causes extraction of oxygen from the matrix of the solid electrolyte, the matrix was depleted of its oxygen only over a very short length of the tube. If the current distribution had been uniform, oxygen would have been extracted locally at a much lower rate when the critical potential was exceeded and the solid electrolyte membrane would have supported the oxygen depletion for a considerably longer operating time than was experienced.

The total current carrying capacity of a solid electrolyte tube membrane approaches an upper limit when the relative length parameter L/L_c reaches the value of approximately 2. This is shown in Figure 10. Any further lengthening of the tube will not increase the capacity of the tube with respect to oxygen extraction. If the electrode design cannot be improved, the maximum length of each tube would be only about 1 cm. The total number of tubes which would be needed for producing 10 kg of oxygen per day would be about 4,000. Still, the electrical power dissipation as shown in Figure 10 would be of such magnitude that the overall efficiency of an oxygen extraction system would make it no longer useful for extraterrestrial oxygen production. In the range of 0 to 2 of the relative length L/L_c, a strong trade-off between number of tubes and overall electrical efficiency can be made realizing that current capacity per tube can only increase with higher electric power dissipation in the electrodes.

2.4 Influence of Contact Resistance

The apparent resistivity of the platinum thick film has been shown to be an order of magnitude higher than would be predicted by basic materials considerations. An additional resistance associated with the electrodes could be a contact resistance which is located between the electrode material and the solid electrolyte. The exact physical behavior of this resistance remains to be investigated.

2.4.1 Analytical Expansion

The analysis as presented above assumed that the electrical circuit includes only two resistive components, the resistance of the membrane and the resistance of the electrodes to current flowing parallel to the membrane surface. Based on this assumption the relation between the applied voltage $2V_o$ and the effective current density i_e could be expressed by relation 31 or

$$2V_o = i_e R_z (L/L_c)/\tanh(L/L_c) \qquad (46)$$

It might, however, be more appropiate to formulate the electrical circuit by the inclusion of a contact resistance which operates in series with the membrane resistance R_z. Relation 46 would then be modified by the inclusion of the contact resistance R_c as shown by relation 47

$$2V_o = i_e (R_z + 2R_c)(L/L_c)/\tanh(L/L_c) \qquad (47)$$

where R_c contact resistance, ohm-cm^2

The characteristic length L_c as was defined by relation 18 has now to be redefined by

$$L_c = \{(R_z + 2R_c)/2R_e\}^{1/2} \qquad (48)$$

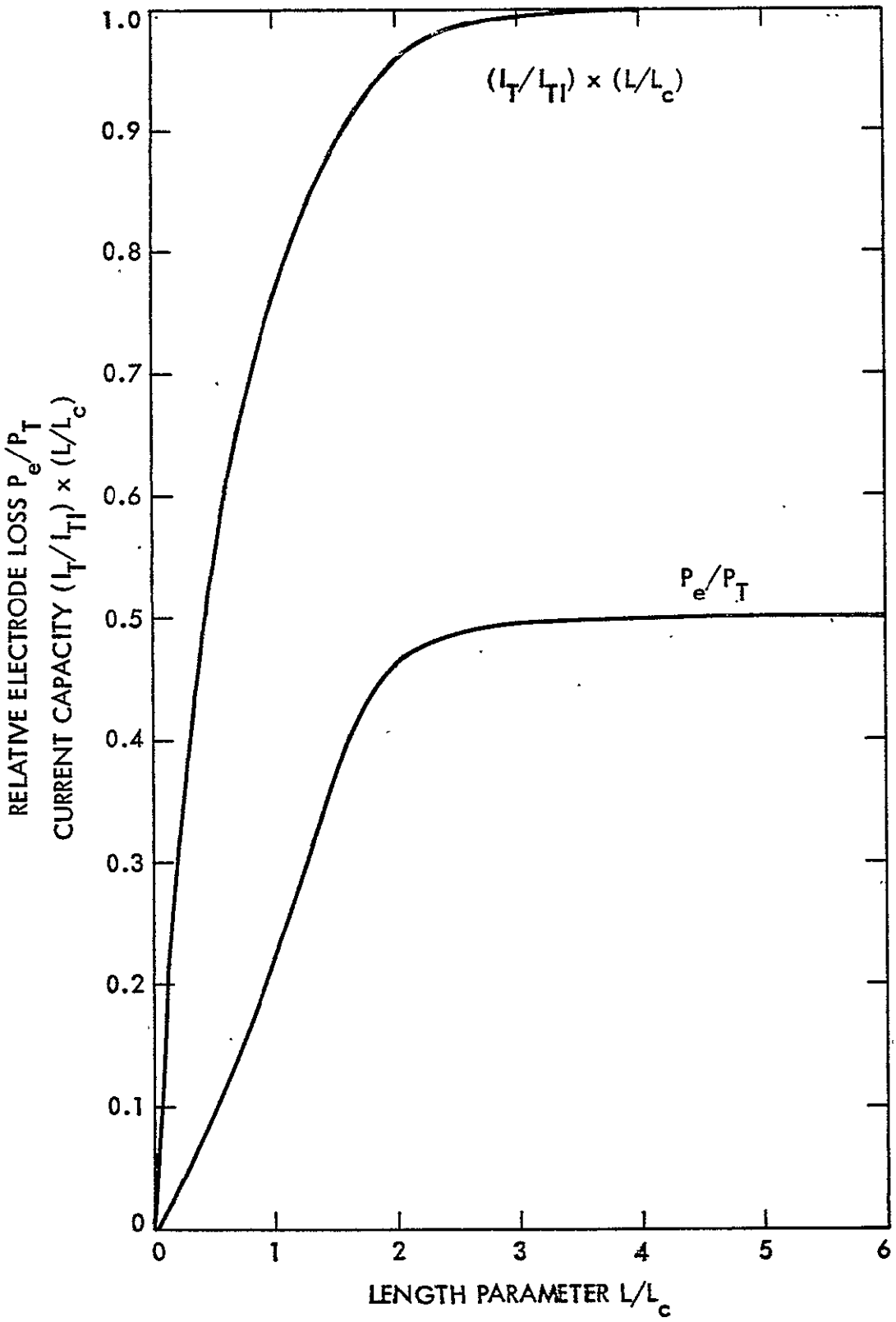

Figure 10 Total Current Carrying Capacity and Relative Electrode Loss

and the length parameter L/L_c thus becomes

$$L/L_c = L\{2R_e/(R_z + 2R_c)\}^{1/2} \tag{49}$$

The total resistance is now the sum of three resistances

$$R_T = R_{se} + R_z + 2R_c \tag{50}$$

The experimentally determined resistance which is attributed to the electrode is now the result of a combination of contact resistance R_c and electrode resistance R_e. These two resistances determine the surface resistance R_{se} as given by the modified relation 32

$$R_{se} = (R_z + 2R_c)\{(L/L_c)/\tanh(L/L_c) - 1\} \tag{51}$$

When relation 51 is inserted into relation 50 the total resistance is

$$R_T = (R_z + 2R_c)(L/L_c)/\tanh(L/L_c) \tag{52}$$

Since from relation 49

$$(R_z + 2R_c) = 2R_eL^2/(L/L_c)^2 \tag{53}$$

the total resistance can also be expressed by

$$R_T = 2R_eL^2/(L/L_c)\tanh(L/L_c) \tag{54}$$

The total current I_T is from relation 28b

$$I_T = \{2V_oLb/(R_z+2R_c)\}\{\tanh(L/L_c)\}/(L/L_c) \tag{55a}$$

and the relative total current, which is the ratio between the actual total current and the current flow through a membrane whose total resistance consists solely of the membrane resistance R_z, is according to relation 28a

$$I_T/(2V_oLb/R_z) = \{R_z/(R_z+2R_c)\}\{\tanh(L/L_c)\}/(L/L_c) \tag{55b}$$

The absolute power loss in the electrodes due to the resistive component of the electrodes is from relation 36

$$P_e = \{(2V_o)^2Lb/2(R_z+2R_c)\}\{[\tanh(L/L_c)]/(L/L_c) - \cosh^{-2}(L/L_c)\} \tag{56a}$$

while the relative power dissipation in the electrodes is

$$P_e/\{(2V_o)^2Lb/R_z\} = \{R_z/(R_z+2R_c)\}\{[\tanh(L/L_c)]/(L/L_c) - \cosh^{-2}(L/L_c)\}/2 \tag{56b}$$

The combined power loss in the membrane and due to contact resistance is the difference between the total power loss and the

resistive power loss in the electrodes

$$P_{zc} = P_T - P_e \tag{57}$$

The total power P_T dissipated is from relations 43 and 55a

$$P_T = \{(2V_o)^2 Lb/(R_z+2R_c)\}\{\tanh(L/L_c)\}/(L/L_c) \tag{58a}$$

while the relative total power dissipation is

$$P_T/\{(2V_o)^2 Lb/R_z\} = \{R_z/(R_z+2R_c)\}\{\tanh(L/L_c)\}/(L/L_c) \tag{58b}$$

When replacing the total power dissipation P_T and the electrode power loss P_e as given by relations 58a and 56a in relation 57, the combined power dissipation in the membrane and due to contact resistance is

$$P_{zc} = \{(2V_o)^2 Lb/(R_z+2R_c)\}\{[\tanh(L/L_c)]/(L/L_c) + \cosh^{-2}(L/L_c)\}/2 \tag{59a}$$

or

$$P_{zc}/\{(2V_o)^2 Lb/R_z\} = \{R_z/(R_z+2R_c)\}\{[\tanh(L/L_c)] + \cosh^{-2}(L/L_c)\}/2 \tag{59b}$$

The power dissipation in the membrane alone is a fraction of the combined power dissipation according to the relative resistance.

$$P_z/\{(2V_o)^2 Lb/R_z\} = \{R_z/(R_z+2R_c)\}^2\{[\tanh(L/L_c)]/(L/L_c) + \cosh^{-2}(L/L_c)\}/2 \tag{60}$$

The power dissipation due to the contact resistance R_c is similarly

$$P_c/\{(2V_o)^2 Lb/R_z\} = \{R_z 2R_c/(R_z+2R_c)^2\}\{[\tanh(L/L_c)]/(L/L_c) + \cosh^{-2}(L/L_c)\}/2 \tag{61}$$

2.4.2 Application to Experimental Data

With the help of relation 54, the combination between the electrode resistance R_e and the contact resistance R_c for the measured total resistance $R_T = 23.73$ ohm-cm^2 can be evaluated as shown in Figure 11.

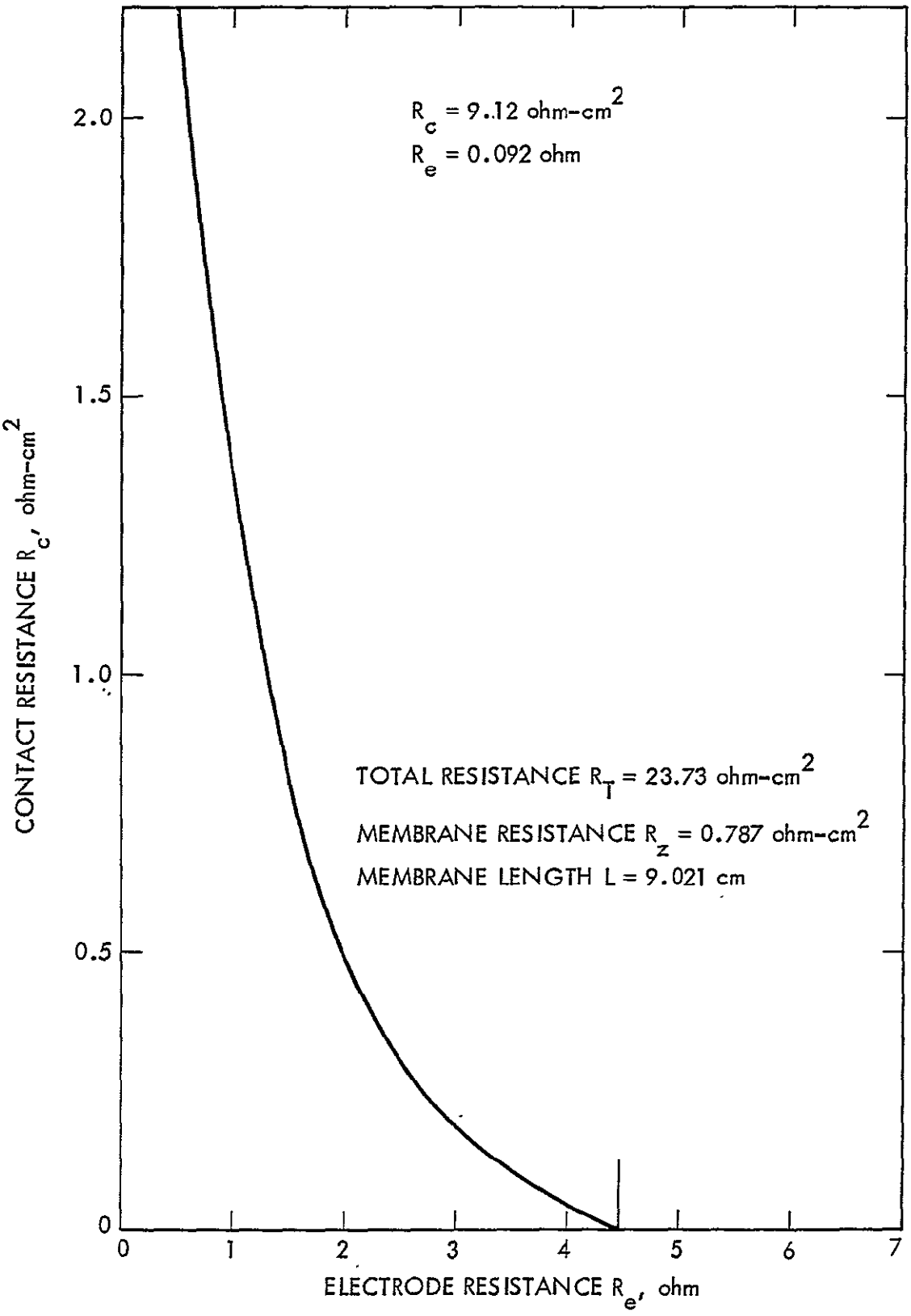

Figure 11 Combinations of Electrode Resistances and Contact Resistances Satisfying Measured Surface Resistance

Two extreme combinations can be considered for the two resistances. One case would assume that the entire resistance associated with the electrodes has to be attributed to the electrode resistance R_e and that contact resistance R_c is negligible. The other extreme case would accept an electrode resistance R_e = 0.092 ohm, which is based on the extrapolated materials properties of the platinum thick film, and attribute the high unaccounted for fraction of the surface resistance entirely to a contact resistance R_c = 9.12 ohm-cm^2. This contact resistance compares with the membrane resistance R_z = 0.787 ohm-cm^2.

For this case the characteristic length L_c would be from relation 48

$$L_c = 10.169 \text{ cm}$$

and the relative length for the tested membrane would be

$$L/L_c = 0.8871$$

The current density distribution along the length of the tube membrane would have been as shown in Table 3. This current density distribution can be compared with the current density distribution presented in Table 2 which was calculated with the assumption of negligible contact resistance.

RZ = .787 OHM-CM2 RE = .092 OHM RC = 9.12 OHM-CM2
L = 9.021 CM

CHARACT.LENGTH L_C	10.169 CM	REL. LENGTH	0.88711
REL.TOTAL POWER	.0331026	REL.ELECTRODE POWER	0.00629
REL.MEMBRANE POWER	0.00111	REL.CONTACT POWER	0.02570

RELATIVE DISTANCE x/L	RELATIVE CURRENT DENSITY
0.0	1.0
.1	.940873
.2	.889155
.3	.844439
.4	.806374
.5	.774658
.6	.749042
.7	.729325
.8	.715351
.9	.707011
1	.704238

Table 3 Current Density Distribution in an Experimental Solid Electrolyte Tube Membrane With Extreme Contact Resistance

It appears to be highly unlikely that the primary cause for the high surface resistance was a contact resistance of R_c= 9.12 ohm-cm^2. The high contact resistance would have resulted in a relatively uniform current density distribution which would have prevented the highly localized reduction of the solid electrolyte membrane material.

Section III

CONCLUSION

The electrical analysis presented in this report has given an insight into the operation of a solid electrolyte membrane oxygen extraction device. It has proven the current density to be non-uniform in a tube solid electrolyte membrane. The major parameter influencing the current density distribution was shown to be a length parameter L/L_c, which is the ratio between the absolute length of the tube and the characteristic length. The characteristic length was found to be a function of all resistances of the components which comprise the solid electrolyte membrane. The derived relations permit an evaluation of the influence of the resistive components in the electric circuit on the performance of an oxygen extraction device. The combined results of the electric analysis and the test data have now clearly proven platinum thick film electrodes to be entirely inappropiate for solid electrolyte devices that operate with current flow.

It would be desirable to perform some basic experiments by which the platinum thick film electrode resistance could be measured directly at high operating temperatures. With the electrode resistance R_e known, the magnitude of the contact resistance R_c could be established. This would be an important investigation as it would clarify whether the effort for lowering the electrode resistance with an integrated electrode will bring about the lowering of the total losses as expected at the present time, or whether a contact resistance R_c is actually the major loss factor, which cannot be lowered or eliminated even with an integrated electrode.

NOMENCLATURE

A	area, cm^2
b	width, cm
I	current, ampere
i	current density, ampere/cm^2
L	length, cm
P	power, watt
R	resistance, ohm
R	resistance, ohm-cm^2
t	thickness, cm
V	voltage drop, volt
V_o	applied potential, volt
v	non-dimensional voltage drop
x	distance, cm
ρ	resistivity, ohm-cm
τ	voltage drop function (relation 12a)

Subscripts

c	characteristic
c	contact
e	electrode
f	film
P	platinum
P	power
s	surface
T	total
V	voltage
x	at distance x

REFERENCES

1. Patent No. 4,331,742

2. Richter, Robert: Basic Investigation into the Production of Oxygen in a Solid Electrolyte Process. AIAA Paper AIAA-81-1175, AIAA 16th Thermophysics Conference, June 23-25, 1981, Palo Alto, California.

3. Strickler, D. W.: Electrical Conductivity in the ZrO_2-Rich Region of Several M_2O_3 - ZrO_2 Systems. J. American Ceramic Soc., Vol. 48, No. 6, pg. 286 (June 1965).